20th Australasian Fluid Mechanics Conference
Perth, Australia
5-8 December 2016

Developing turbulent boundary layers with spanwise periodic trips

R. Baidya[1], C. M. de Silva[1], Y. Huang[1], L. Castillo[2], I. Marusic[1] and N. Hutchins[1]

[1]Department of Mechanical Engineering
The University of Melbourne, Victoria 3010, Australia

[2]Department of Mechanical Engineering
Texas Tech University, Lubbock, TX 79409-1021, United States of America

Abstract

Our work builds on the investigation of Marusic et al. [7] who examined the streamwise evolution of a turbulent boundary layer from different types of spanwise homogeneous trips. Here we introduce a spanwise three dimensionality at the trip by employing a series of miniature vortex generators placed immediately downstream of the original spanwise homogeneous trip in a high Reynolds number boundary layer facility. The resultant modified boundary layer is surveyed using hot-wire anemometry to examine its streamwise evolution. Further, a series of targeted Particle Image Velocimetry measurements are conducted to examine the modified structural composition of the flow. The results exhibit the presence of streamwise counter-rotating roll-modes over a large streamwise extent, which appear to be strongest after a certain characteristic length downstream of their introduction. Comparisons are drawn between the observed evolution of a turbulent boundary layers with a spanwise three dimensionality and the evolution model of Perry et al. [8], which is formulated for spanwise homogeneous flows. Preliminary findings reveal that the spanwise periodic modes introduced at the inception point (trip) of a turbulent boundary layer can persist for a substantial streamwise extent. Further, even at the furthest downstream station surveyed ($x > 1000$ vortex generator heights) little or no recovery towards the canonical state was observed for some evolution parameters, perhaps suggesting that three-dimensionality can alter the asymptotic state, or at least significantly delay recovery to the canonical state.

Introduction

The evolutionary characteristics of turbulent boundary layers are of significant engineering interest. From a practical perspective, an accurate model of the evolution enables the estimation of parameters such as the net drag force, based only on a knowledge of the flow at some initial condition as an input [8]. Marusic et al. [7] have investigated the evolution of turbulent boundary layers under different tripping conditions, demonstrating that different inlet conditions can alter the evolution for substantial development lengths, and also showing that the model of Perry et al. [8] can provide accurate predictions even with modified inlet conditions, given a sufficient empirical closure model. The work of Marusic et al. [7] also showed that, asymptotically, the evolution of the turbulent boundary layer tended to a canonical state with sufficient development length, if the tripping / inlet conditions are two dimensional. It should be noted that, the conclusions drawn by Marusic et al. [7] were based on streamwise velocity statistics, however evidence exists to suggest that recovery in the wall-normal variance and Reynolds shear stress are significantly slower. For example, Seo et al. [9] find cases where the wall-normal variance and Reynolds shear stress have not recovered to the canonical state in excess of 30 m, or $O(10^4)$ trip heights, downstream of the trip.

All of the trips investigated by Marusic et al. [7] were spanwise homogeneous (effectively different sized trip rods). However, there is evidence in the literature that spanwise inhomogeneity in the free-stream occurring over some large wavelength, can introduce unusually persistent features into the developing turbulent boundary layer [2, 12]. In fact, it has been reported that small lateral variations at the origin of boundary layers tend to be selectively amplified up to a critical amplitude as the boundary layer develops [11], with the most amplified or dominant wavelengths tending to be those that are on the order of the layer thickness. Based on these results, we here propose to extend the study of Marusic et al. [7], using three-dimensional, spanwise periodic trips to introduce lateral variations at the origin of the turbulent boundary layer. The aim here is to generate persistent modes that in turn may offer a more gradual evolution towards the canonical state. Underpinning this study is the question of whether the evolution of the turbulent boundary layer can be tweaked efficiently at the trip, such that eventually some net performance advantage might be attained. This initial study investigates vortex generators to introduce the spanwise variations in the tripped layer. These data will then inform the development of dynamic trips for future studies.

Experimental Set-up

The experiments are performed at the High Reynolds Number Boundary Layer Wind Tunnel (HRNBLWT) at the University of Melbourne. Figure 1 shows an overall view of the experimental campaign, which employs both hot-wire anemometry and particle image velocimetry (PIV) measurements. Typically, the boundary layer in the facility is tripped using a strip of 40 grit sand paper (SP40); and this will correspond to our reference case. For the present study, spanwise-periodic modes are introduced using a series of miniature vortex generators (MVGs) that are positioned immediately downstream of the SP40 trip. The parameters chosen for the MVG geometry were initially based on study of Shahinfar et al. [10]. However, to ensure a measurable boundary layer modification was present in excess of 5 m downstream from the MVG trip the spanwise wavelength (Λ), height and length was increased to 216, 14 and 75 mm, respectively (cf. figure 1, inset A). To put this in context, the incoming boundary layer thickness onto the MVGs is 20 mm.

For the preliminary results presented here, the hot-wire measurements are performed using an autonomous traverse which translates in both the streamwise and wall-normal directions. The hot-wire sensor consists of a 5 µm diameter platinum wire, operated using a Melbourne University Constant Temperature Anemometer. To systematically examine the modified boundary layer we perform wall-normal surveys of the flow at a series of streamwise positions downstream (at x =1, 2, 5, 7 and 13 m) from the periodic trip. Such an examination is made possible by the large developing length (27 m) of the boundary layer in the working section, which gives an opportunity to draw comparisons to the reference flow over a large spatial extent and large Reynolds number range.

The PIV experiments are targeted in nature and are conducted at a streamwise position where the largest flow modifications were observed from the hot-wire measurements. Specifically, the imaging system is oriented to acquire streamwise-spanwise vector fields at several heights across the boundary layer. We utilise two PCO4000 cameras (4008×2672 pixels, 2Hz) equipped with 60 mm Nikon lens to obtain a field of view of approximately $0.3\,\mathrm{m} \times 0.25\,\mathrm{m}$, or $3.5\delta \times 2.5\delta$, where δ corresponds to the local boundary thickness, defined here as the wall-normal location where the mean velocity is 99% of the free-stream velocity, U_∞.

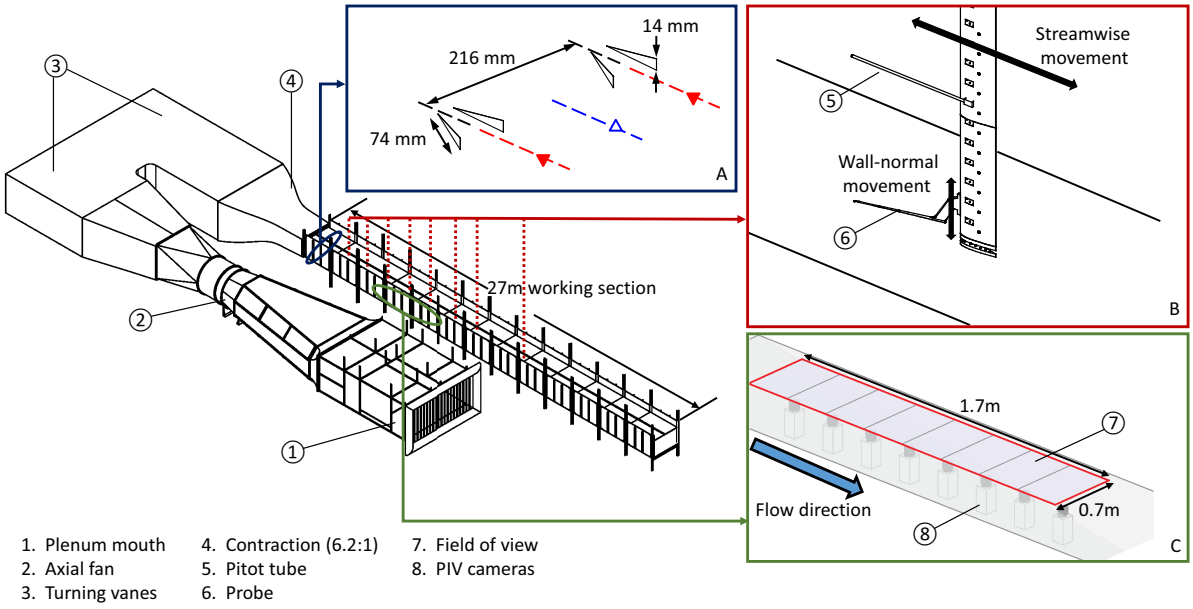

Figure 1: Overview of experimental campaign, adapted from Baars et al. [1]. The vertical dashed lines indicate streamwise location of the measurement stations. The insets A-C illustrate the micro vortex generators (MVG), hot-wire traverse system and the particle image velocimetry system. In inset A, ▵ and ▼ denote the common flow up and down regions.

The flow is illuminated by a laser sheet generated by a Spectra Physics 'Quanta-Ray' PIV 400 Nd:YAG double-pulse laser that delivers 400 mJ/pulse. The experimental data are processed using an in-house PIV package, with an interrogation window size of 32×32 pixels, which corresponds to approximately 25 viscous units for the reference boundary layer [5].

In this paper, x, y and z indicate the streamwise, spanwise and wall-normal directions. The total streamwise velocity is denoted by $\tilde{U}$, while U and u correspond to the local mean velocity at a particular spanwise location and fluctuations about that local mean velocity, respectively (i.e. $\tilde{U} = U + u$).

Results

Figure 2 shows how U develops downstream of the MVG. The profiles are ordered vertically with the distance from the trip increasing from top to bottom. The three-dimensionality introduced by the MVG results in non-uniform statistics in the spanwise (y) direction. To examine this non-uniformity the symbols ▵ and ▼ will be used to represent the region directly behind a pair of MVG blades and the mid-point between two MVGs, respectively (cf. figure 1, inset A). Further, the solid line corresponds to the reference profile with a the SP40 trip (referred to hereafter as the canonical case). Relative to the canonical case, the flow behind a pair of MVG blades and mid-point of two MVGs is respectively slower and faster. This subsequently leads to a higher local boundary layer thickness relative to the canonical profile along ▵, while the opposite occurs along ▼. Such a scenario is evident in the mean flow statistics shown in figure 2, and is also consistent with a presence of counter-rotating streamwise roll-modes with a common flow up along ▵ and a common flow down along ▼ [6].

Since the spanwise three dimensionality introduced by the MVG trip leads to a departure from Perry's model [8], we use the model as a measure of the streamwise extent of the modification introduced. To this end, figures 3(a-d) show comparisons of the evolution parameters from the experiments (symbols) and the model (dashed and dotted lines). We note that the model predictions are based on initial parameters at $x = 1$ and 5 m. Further, the parameters shown in figures 3(a-d) (including C_f) have been computed by fitting a composite profile [3] to the experimental data. This ensures that parameters are defined consistently across all profiles and minimises the influence of discretisation (in z locations) and measurement uncertainty in the experimental data.

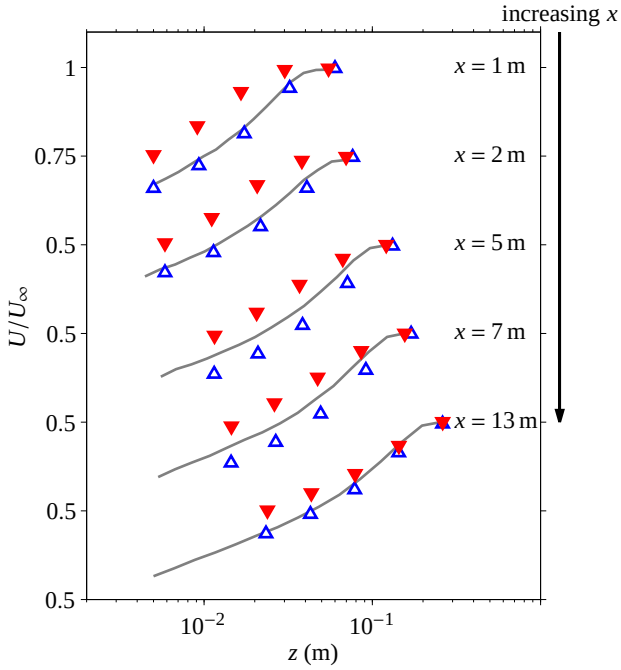

Figure 2: Comparison of streamwise mean velocity statistics at five streamwise locations. The symbols correspond to velocity profiles in the common flow up (▵) and down (▼) regions, while the solid line denote the canonical profile.

The composite fits used to evaluate the evolution parameters show in figure 3 for the MVG cases only have a total of five wall-normal logarithmically spaced points across the entire wall-normal extent of the boundary layer, while the canonical case (cf. solid lines in figures 3a-d) has a total of 15 logarithmically spaced points. To ensure that the lower number of grid points available for the MVG cases has negligible impact on the evolution parameters computed, the ▲ and ▼ symbols in figures 3(a-d) correspond to results computed from a velocity profile with 25 logarithmically spaced wall-normal locations at $x = 5$ for the common flow up and down cases, respectively. Good agreement observed between the parameters calculated from sparse and detailed traverses suggest that the sparse traverses sufficiently capture the evolution of these parameters as a function of development distance. The vertical error bars in figure

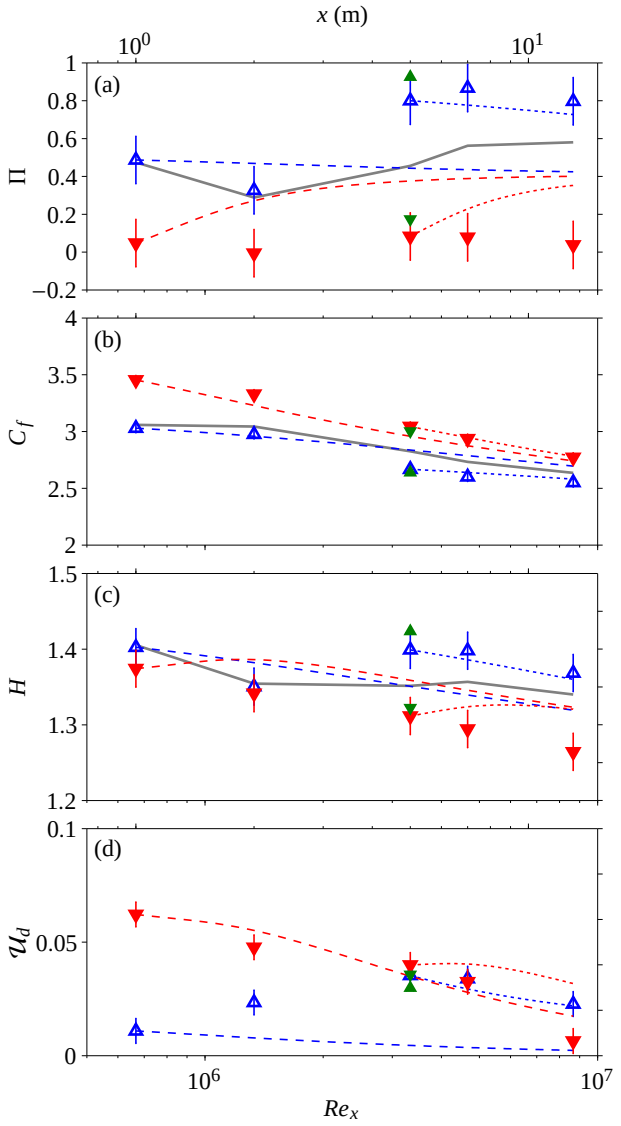

Figure 3: Comparison of boundary layer parameters from experiments and computed evolution. (a) Π vs. Re_x, (b) C_f vs. Re_x, (c) H vs. Re_x and (d) $\mathcal{U}_d$ vs. Re_x. The symbols correspond to evolution in the common flow up (△) and down (▼) regions, while the solid line denote evolution for the canonical case. The dashed (- - , - -) and dotted (· · · , · · ·) lines correspond to the computed evolution following Marusic et al. [7] and Perry et al. [8], initialised based on the experimental parameters at $x = 1$ and 5 m.

3 correspond to the maximum deviation observed between the the sparse and detailed profiles.

Figure 3(a) shows how the wake factor, Π, varies with Reynolds number based on development distance ($Re_x = xU_\infty/\nu$). Figures 3(b-d) show the streamwise variation of the skin friction coefficient, shape factor (H), and the integrated difference in the velocity profiles ($\mathcal{U}_d$) versus Re_x. Here, $H = \delta^*/\theta$ where δ^* and θ respectively correspond to the displacement and momentum thickness. Further, $\mathcal{U}_d = \left|\int_0^\infty (U - U_s)/U_\infty \, d\eta\right|$, where $U - U_s$ is the difference in the mean velocity between the MVG and the canonical case, while $\eta = z/\delta_s$. Comparison of the actual (△, ▼) and predicted (- - , · · ·) evolution suggests that not all boundary layer parameters are equally sensitive to spanwise homogeneity criteria. Specifically, ours results show that while C_f deviates less from their canonical development, Π, H and $\mathcal{U}_d$ show substantial variation. In fact, the modification of Π and H appear to persist beyond $x > 13$ m or $O(10^3)$ MVG heights, reaffirming the longevity of the spanwise periodic modes introduced at the inception (trip) of the turbulent boundary layer.

Figure 3(d) shows that the differences between the mean velocity profiles in the common flow up region and canonical case initially increases before the two profiles approach each other beyond $x > 5$ m. Meanwhile in the common flow down region, $\mathcal{U}_d$ is observed to monotonically approach zero with increasing x. Although not reproduced here, our findings also show that the spanwise wavelength of the MVG trip, Λ, appears to significantly impact the location where the maximum deviation occurs. For the case presented in figure 3(d), the maximum deviation occurs at $x \sim 5$ m, which coincides with the location where the ratio between Λ and the local δ is approximately equal to two. Therefore, we postulate that the boundary layer appears to be selectively amplifying spanwise periodic modes of $O(\delta)$, however, further measurements are necessary (and will be undertaken) to examine this behaviour.

Figures 4(a-b) present instantaneous velocity fields obtained using PIV for the canonical and modified turbulent boundary layer respectively. The colour contours represent streamwise velocity on a xy plane, at a wall-normal height of $z/\delta_s \approx 0.4$ located approximately 5 m (or 350 MVG heights) from the trip. Qualitatively, the periodicity introduced by the MVG has generated an underpinning large-scale counter rotating roll-mode, somewhat similar to that observed on certain rough wall flows (e.g. converging/diverging riblets) [6]. Thus, we may expect similar preferential alignment of structures within the modified boundary layer to that observed on certain rough-walled flows. For example, figure 4(b) shows meandering large-scale low- and high-speed structures present in the common flow down (red dashed) and up (blue dashed) regions, respectively. Although not shown here, these observations are repeatable in almost all PIV frames captured. Therefore, the present work highlights that the signature of the MVG trip is present over a large spatial extent, highlighting the potential to selectively tune turbulent structures by means of modifying boundary layer inlet conditions.

To further elucidate these observations, figure 4(c) shows the mean velocity computed as a function of y and z, where the spanwise periodicity is present across the entire extent of the boundary layer. Eventually, further targeted inspections using PIV will allow us to compute the total integrated difference across one complete spanwise period to compliment the single point measurements taken only at selected spanwise positions, but over a large streamwise extent. Figure 5 shows the normalised two-point correlation function for the streamwise velocity (R_{uu}) for the canonical and modified boundary layers at $z/\delta_s \approx 0.4$. We note that the velocity fluctuations are computed relative to the local mean due to the spanwise inhomogeneity for the modified turbulent boundary layer [4]. The results show that the flow modification introduced by the MVGs have oriented the coherent regions of $\overline{U}$ away from the common flow up region. On the other hand, the canonical boundary layer shows no preferential alignment. Although not reproduced here these difference seem to be prevalent at only particular wall-normal positions, therefore we may infer that a dynamic MVG-type system may be used to intelligently target and modify the structural arrangement in boundary layers in particular regions, which will be the subject of our future work.

Summary and conclusions

The wall-parallel PIV fields exhibited the presence of streamwise roll-modes downstream of the vortex generators. Furthermore, hot-wire anemometry surveys revealed that the influence of the introduced spanwise periodicity at the origin of the boundary layer is largest after a certain characteristic length downstream. This is in contrast to the evolution behind a two dimensional trip, which approaches an asymptotic behaviour towards the canonical boundary layer much earlier. These differences are thought to originate from the interaction between the large-scale spanwise modes and the boundary layer. Ultimately, understanding of these interactions gained from this study will

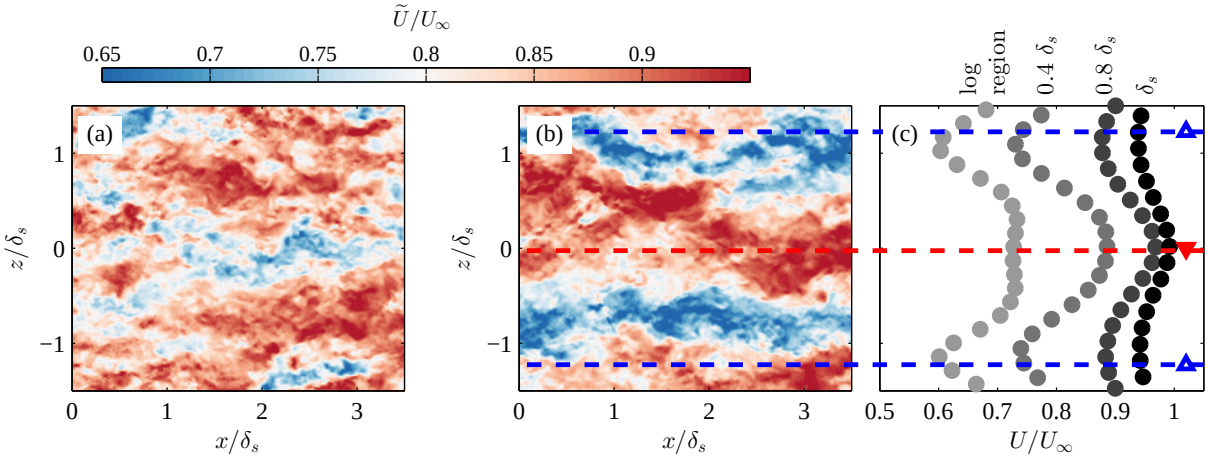

Figure 4: (a) and (b) show colour contours of instantaneous streamwise velocity for the canonical and modified (MVG trip) turbulent boundary layer, respectively. (c) Spanwise variation of streamwise mean flow for MVG trip flow. Shading levels of the ● symbols correspond to wall-normal height. The red and blue dashed lines in (b-c) correspond to the common flow down and up regions.

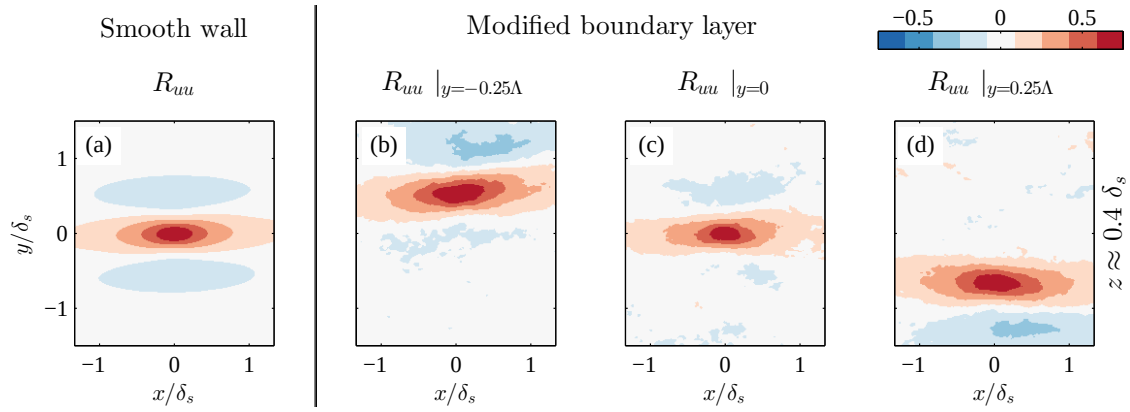

Figure 5: Wall-parallel planes of the normalised two-point correlation for the streamwise velocity (R_{uu}) for the (a) canonical boundary layer and (b-d) modified boundary layer using MVG trip. Results are presented at a wall-normal height of $z \approx 0.4\delta_s$. (b-d) correspond to spanwise locations $y/\Lambda = -0.25, 0$ and 0.25, respectively.

be used in an attempt to intelligently introduce a spanwise dynamical perturbations at the origin of the boundary layer, to modify its evolution.

Acknowledgement

The authors would like to acknowledge the Australian Research Council and the Office of Naval Research (Global) for financial support.

References

[1] Baars, W. J., Squire, D. T., Talluru, K. M., Abbassi, M. R., Hutchins, N. and Marusic, I., Wall-drag measurements of smooth-and rough-wall turbulent boundary layers using a floating element, *Exp. Fluids*, **57**, 2016, 1–16.

[2] Bradshaw, P., The effect of wind-tunnel screens on nominally two-dimensional boundary layers, *J. Fluid Mech.*, **22**, 1965, 679–687.

[3] Chauhan, K. A., Monkewitz, P. A. and Nagib, H. M., Criteria for assessing experiments in zero pressure gradient boundary layers, *Fluid Dyn. Res.*, **41**, 2009, 021404.

[4] Coceal, O. and Belcher, S. E., A canopy model of mean winds through urban areas, *Q. J. R. Meteorolog. Soc.*, **130**, 2004, 1349–1372.

[5] de Silva, C. M., Squire, D. T., Hutchins, N. and Marusic, I., Towards capturing large scale coherent structures in boundary layers using particle image velocimetry., in *Proc. 6th Aust. Conf. Laser Diag. Fluid Mech. Comb.*, University of Melbourne, 2015.

[6] Kevin, Nugroho, B., Monty, J. P. and Hutchins, N., Wall-parallel PIV measurements in turbulent boundary layers with highly directional surface roughness, in *Proc. 19th Aust. Fluid Mech. Conf.*, 2014.

[7] Marusic, I., Chauhan, K. A., Kulandaivelu, V. and Hutchins, N., Evolution of zero-pressure-gradient boundary layers from different tripping conditions, *J. Fluid Mech.*, **783**, 2015, 379–411.

[8] Perry, A. E., Marusic, I. and Li, J. D., Wall turbulence closure based on classical similarity laws and the attached eddy hypothesis, *Phys. Fluids*, **6**, 1994, 1024–1035.

[9] Seo, J., Castillo, L., Johansson, T. G. and Hangan, H., Reynolds stress in turbulent boundary layers at high Reynolds number, *J. Turbul.*, **5**, 2004, 13–13.

[10] Shahinfar, S., Fransson, J. M., Sattarzadeh, S. S. and Talamelli, A., Scaling of streamwise boundary layer streaks and their ability to reduce skin-friction drag, *J. Fluid Mech.*, **733**, 2013, 1–32.

[11] Townsend, A. A., *The structure of turbulent shear flow*, Cambridge Univ Press, Cambridge, UK, 1976.

[12] Watmuff, J. H., Detrimental effects of almost immeasurably small freestream nonuniformities generated by wind-tunnel screens, *AIAA Journal*, **36**, 1998, 379–386.